

## Interplay between Kondo-like behavior and short-range antiferromagnetism in $\text{EuCu}_2\text{Si}_2$ single crystals

C. D. Cao,<sup>1,2</sup> R. Klingeler,<sup>1</sup> N. Leps,<sup>1</sup> H. Vinzelberg,<sup>1</sup> V. Kataev,<sup>1</sup> F. Muranyi,<sup>1</sup> N. Tristan,<sup>1</sup> A. Teresiak,<sup>1</sup> Shengqiang Zhou,<sup>3</sup> W. Löser,<sup>1</sup> G. Behr,<sup>1</sup> and B. Büchner<sup>1</sup>

<sup>1</sup>Leibniz-Institut für Festkörper- und Werkstofforschung (IFW) Dresden, Postfach 270116, D-01171 Dresden, Germany

<sup>2</sup>Department of Applied Physics, Northwestern Polytechnical University, Xi'an 710072, People's Republic of China

<sup>3</sup>Institute for Ion Beam Physics and Materials Research, Forschungszentrum Dresden-Rossendorf, P.O. Box 510119, 01314 Dresden, Germany

(Received 21 January 2008; revised manuscript received 25 June 2008; published 12 August 2008)

The static and dynamic magnetic properties, electrical resistivity, specific heat, and magnetoresistance have been studied in  $\text{EuCu}_2\text{Si}_2$  single crystals grown by a floating zone method. The magnetic susceptibility exhibits a considerable anisotropy and a steep rise below 10 K for external fields parallel to the  $c$  axis but with no evident magnetic ordering in the temperature range of 2–350 K. The data imply a gradual change in the Eu valence as a function of temperature. Electron spin resonance (ESR) measurements reveal a sizeable fraction of stable  $\text{Eu}^{2+}$  magnetic moments that interact with conduction electrons and develop quasistatic antiferromagnetic correlations on the ESR timescale. The electrical resistivity and specific heat demonstrate the presence of spin fluctuations and Kondo-like behavior, which apparently competes with the antiferromagnetic order. The analysis of experimental data enables to conclude that the remarkable diversity of the physical properties of  $\text{EuCu}_2\text{Si}_2$  results from the variation of lattice parameters as well as of local crystal chemistry as a consequence of the particular preparation route employed for the growth of single crystals and polycrystals.

DOI: 10.1103/PhysRevB.78.064409

PACS number(s): 75.50.Ee, 75.30.Mb, 72.15.Qm

### I. INTRODUCTION

The large class of  $RT_2\text{Si}_2$  ( $R$ =rare earth,  $T$ =transition metal) intermetallic compounds crystallizing in  $\text{ThCr}_2\text{Si}_2$ -type body-centered tetragonal structure shows interesting magnetic and electric transport properties.<sup>1,2</sup> Among these compounds  $\text{EuCu}_2\text{Si}_2$  is an ideal subject for studying charge configuration fluctuations.<sup>2–11</sup> Polycrystalline  $\text{EuCu}_2\text{Si}_2$  samples exhibit a large magnetic susceptibility but with no magnetic order transition, a large electronic specific-heat coefficient, and deviations from a conventional temperature law in the resistivity.<sup>2,3</sup> The effective valence of the Eu is gradually reduced from about +2.8 at low temperature (2 K) to +2.6 at room temperature (300 K).<sup>3,4,6</sup>

Because of the high-vapor pressure of Eu so far,  $\text{EuCu}_2\text{Si}_2$  single crystals have been grown only by a flux method using indium as melt flux.<sup>12</sup> From these crystals antiferromagnetic ordering below  $T_N=10$  K and a considerable anisotropy of the magnetic properties parallel and perpendicular to the  $c$  axis have been deduced. The  $c$  axis ( $\langle\langle 001 \rangle\rangle$ ) represents the magnetic easy axis. In Ref. 13, for crystals prepared with the same method, two magnetic transitions at 10 and 4 K and exotic electrical properties below  $T=2$  K were reported. This behavior and the magnetic properties of the single crystals turned out to be at strong variance with those of polycrystalline samples, which do not show evidence of magnetic order.<sup>3,11</sup> For a related compound  $\text{YbNi}_2\text{Si}_2$ , Bud'ko *et al.*<sup>14</sup> reported a sensitive dependence of the electrical and magnetic properties on the preparation route of crystals grown by two alternative methods, from an indium flux and from a self-flux, respectively. So far, no information has been available on the physical properties of  $\text{EuCu}_2\text{Si}_2$  single crystals grown from a self-flux.

In order to throw more light on the physical properties of the  $\text{EuCu}_2\text{Si}_2$  compound, magnetic and electrical properties

have been studied in the present work on a single crystal prepared by a floating zone (FZ) method. Here the molten zone acts as a self-flux, which considerably differs from the In flux used by previous authors.<sup>12,13</sup> As a consequence of the different preparation route, we have found distinct magnetic and transport properties of our samples, which can be understood as interplay between a Kondo-like behavior and antiferromagnetic correlations between stable  $\text{Eu}^{2+}$  magnetic moments at low temperatures. This paper is organized as follows: In Sec. II the preparation method and experimental details are presented. Magnetic, thermodynamic, electron spin resonance (ESR), and transport measurements are described in Sec. III. Section IV is devoted to the discussion of the obtained results, which is followed by conclusions in Sec. V.

### II. EXPERIMENT

The  $\text{EuCu}_2\text{Si}_2$  single crystals have been grown by a FZ technique with radiation heating in a vertical double ellipsoid optical configuration with a 5 kW air-cooled xenon lamp positioned at the focal point of the lower mirror. A coarse-grained  $\text{Eu}_{20.5}\text{Cu}_{39.5}\text{Si}_{40}$  feed rod with excess Eu—prepared from high-purity elements 99.98 wt % Eu, 99.999 wt % Cu, and 99.9999 wt % Si—was utilized to balance evaporation losses. The growth process proceeded with a growth velocity of 3 mm/h in a vacuum chamber under elevated pressure (3.5 MPa) of flowing Ar in order to limit severe evaporation losses of the melt. Two  $\text{EuCu}_2\text{Si}_2$  single crystals, 6 mm in diameter and up to 20 mm length, have been obtained. The crystals grew with a preferred orientation close to  $a$  axis ( $\langle\langle 100 \rangle\rangle$ ) with about  $15^\circ$  deviation from the rod axis as determined by the x-ray Laue back-scattering method. Microstructure and crystal perfection were examined by optical

metallography and scanning electron microscopy.<sup>15</sup>

All cuboids and rod-shaped single crystal specimens (with  $a$  and  $c$  as rod axes) employed in the present studies have been cut from the same crystal prepared. Here we only refer to measurements of as-grown single crystalline specimens because annealing at 850 °C for 192 h has only minor effects on physical properties. Magnetic-susceptibility  $\chi(T)$  measurements in the presence of a magnetic field ( $H$ ) of 0.1 T have been carried out in the temperature interval of 2 to 300 K with a quantum design MPMS superconducting quantum interference device magnetometer. In addition, electrical resistivity ( $\rho$ ) measurements have been accomplished in a temperature range of 1.8 to 300 K and in the presence of magnetic fields up to 10 T in an Oxford magnet system by a conventional four-probe method utilizing silver paint for making electrical contacts of the leads with the sample. The specific heat has been measured by means of a Quantum Design PPMS. Electron spin-resonance measurements have been performed with a Bruker EMX spectrometer at a frequency of 9.5 GHz in a temperature range of 3.5–300 K.

### III. RESULTS

#### A. Magnetic properties

##### 1. Static magnetization

In Fig. 1, the magnetic susceptibility  $\chi=M/H$  for the three crystal orientations  $H\parallel c$ ,  $H\parallel a$ , and  $H\parallel b$  ( $\langle\langle 010 \rangle\rangle$ ) is shown. It is found that the annealing treatment has little effect on magnetic susceptibility of this single crystal. The magnetic susceptibility for  $H\parallel a$  and  $H\parallel b$  is nearly identical, which is also demonstrated by the inset showing the inverse susceptibility data. There is, however, a great anisotropy of the magnetic properties between an orientation in the basis plane ( $a, b$ ) and in the perpendicular direction ( $c$ ). The magnetic easy axis is along the  $c$  axis where the magnetic susceptibility displays a sharp increase upon cooling below 50 K, whereas there are only small changes for  $H\parallel a$  and for  $H\parallel b$ . In the crystal at hand, there is no evidence for a long-range magnetic ordering in the temperature range investigated. We mention that there is an additional feature in  $\chi^{-1}(T)$  below  $\sim 10$  K as indicated in Fig. 1(c). Interestingly, the inverse susceptibility  $\chi^{-1}(T)$  fails to show a linear Curie-Weiss law in the range from 2 K to room temperature [Fig. 1(b)]. This behavior reflects the well-known valence fluctuations of  $\text{EuCu}_2\text{Si}_2$ ,<sup>3,4,16</sup> which has been observed for other Eu-containing compounds too.<sup>17</sup> In particular, one expects a Curie-Weiss law of the magnetic susceptibility if the magnetism is governed by a stable magnetic moment associated with a stable Eu valence state. In contrast, the nonlinear temperature dependence of the magnetic susceptibility observed in a variety of materials was straightforwardly attributed to valence fluctuations of the rare-earth ion.

We mention that our data are in a stark contrast to recent data on flux-grown  $\text{EuCu}_2\text{Si}_2$  single crystals, where  $\chi(T)$  for  $H\parallel c$  exhibits a pronounced maximum at  $T_N=10$  K (indicating the onset of antiferromagnetic order) and where  $\chi^{-1}(T)$  is linear over a wide temperature range.<sup>12</sup> The latter observation points to a stable Eu state in that compound. This has

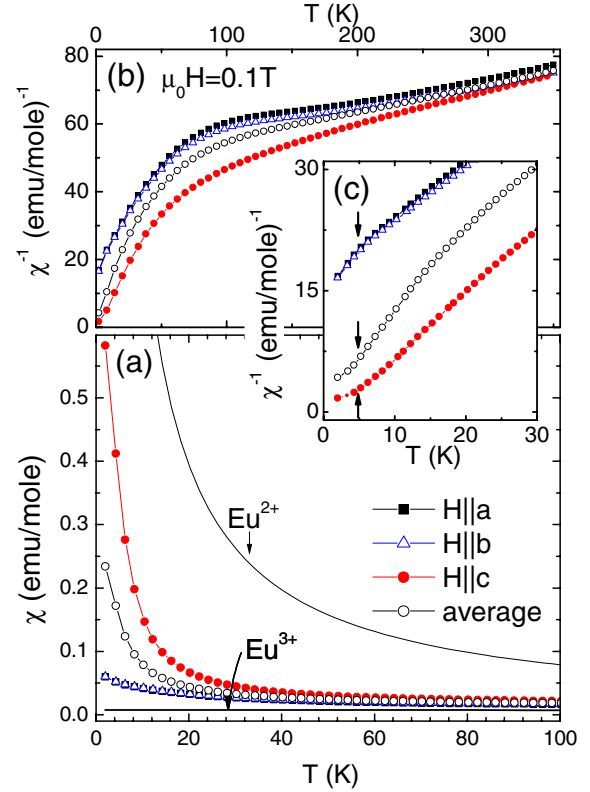


FIG. 1. (Color online) (a) Magnetic susceptibility  $\chi(T)$  as a function of temperature ( $<100$  K) of single crystalline  $\text{EuCu}_2\text{Si}_2$  measured in a magnetic field of 0.1 T for three orientations  $H\parallel a$ ,  $H\parallel b$ , and  $H\parallel c$ . The open circles represent the powder average of the susceptibility. In addition, the response of noninteracting  $\text{Eu}^{2+}$  moments and of  $\text{Eu}^{3+}$  is shown (data from Ref. 4). (b) Corresponding inverse susceptibility  $\chi^{-1}(T)$ . (c)  $\chi^{-1}(T)$  at low temperatures. Arrows indicate additional changes (see the text). Note that the data for  $H\parallel a$  and  $H\parallel b$  are indistinguishable in (a).

been confirmed by recent Mössbauer data, which prove that Eu is in the divalent state in the temperature range of 2–300 K in  $\text{EuCu}_2\text{Si}_2$  single crystals grown from In flux.<sup>18</sup>

It has been shown earlier, e.g., in Ref. 4, that the average susceptibility can be used to monitor quantitatively the temperature dependence of the average valence of the Eu ions by simply interpolating between the  $\text{Eu}^{2+}$  and  $\text{Eu}^{3+}$  susceptibility curves at temperatures above the intrinsic fluctuation temperature. Figure 1(a) shows that the experimental data are in between the susceptibilities of  $\text{Eu}^{3+}$  (data taken from Ref. 4) and noninteracting  $\text{Eu}^{2+}$  moments. Following this method as described in detail, e.g., in Ref. 4, the data imply Eu valence changes from  $\sim 2.53$  at 50 K to  $\sim 2.84$  at 300 K. Note that these values do not change significantly but amount to  $\sim 2.58$  and  $\sim 2.89$ , respectively, if—instead of a Curie law—the Curie-Weiss law with the paramagnetic Weiss temperature  $\theta_p=-18$  K found in Ref. 12 is used for estimating the susceptibility of  $\text{Eu}^{2+}$  as an upper limit. A substantial anisotropy of the magnetic susceptibility for  $H\parallel c$  and  $H\perp c$  is difficult to reconcile with the  $\text{Eu}^{2+}$  paramagnetism, which is of the pure spin nature.

In order to discuss the magnetic properties more in detail, we show in Fig. 2 the magnetization vs external magnetic

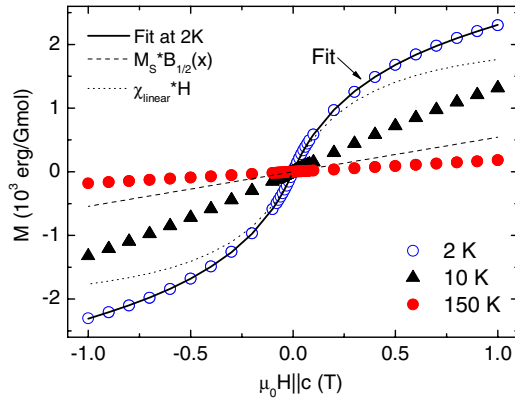


FIG. 2. (Color online) Magnetization vs external magnetic field parallel to the  $c$  orientation of  $\text{EuCu}_2\text{Si}_2$  single crystal  $M(H)$  for selected temperatures 2, 10, and 150 K. The straight line is a fit to the data at 2 K with a linear (dashed line) and a Brillouin-type (dotted line) contribution (see the text).

field for three selected temperatures. Here, the magnetic field has been applied parallel to the  $c$  axis. A first approach to a data analysis is to discuss the magnetization for  $H \parallel c$  at 2 K in terms of a Brillouin function  $B_{1/2}(x)$  (cf. Ref. 19). Interestingly, in addition to the Brillouin function (which reflects the alignment of paramagnetic moments saturating at  $M_S \sim 2100$  emu G/mole) and a small internal field of  $\lambda M_S \sim 2.4$  T (with the mean-field parameter  $\lambda$ ), a considerable linear term  $\chi_{\text{lin}} \sim 0.054$  emu/mole has to be added in order to describe the data. In particular, the saturation value  $M_S$  is strongly reduced with respect to the magnetic moment, which is expected for  $\text{Eu}^{2+}$ . In addition,  $\chi_{\text{lin}}$  is larger than expected from the Van-Vleck magnetism of  $\text{Eu}^{3+}$ . This analysis hence indicates that the upturn in  $\chi(H \parallel c)$  found upon cooling [Fig. 1(a)] at low temperatures is dominated by a Curie-type contribution  $M^{\text{Brill}}(0.1 \text{ T})/H \sim 0.53$  emu/mole, but there is an additional effect reflected by  $\chi_{\text{lin}}$ .

2. ESR measurements

ESR measurements have been carried out in the temperature range of 3.5–300 K at 9.5 GHz with an external magnetic field  $H \parallel c$  axis as shown in Figs. 3 and 4. Above 10 K a single resonance line is observed, which is a field derivative to the absorbed microwave power  $dP(H)/dH$  (representative spectra are shown in Fig. 4). The line shape is asymmetric, which is typical for magnetic ions embedded in metallic environment with the asymmetry parameter  $A/B$  [ratio of the positive and the negative peaks of the  $dP(H)/dH$  curve] of about 1.6. The line can be fitted with a Dysonian function, which describes an ESR response in metals.<sup>20</sup> The linewidth and the resonance field (the  $g$  factor) of the observed ESR line are obtained from Dysonian fits. The inset to Fig. 3 shows the measured ESR line at 25 K together with a respective fit. The difference between the measured and simulated line around 0.1 T is due to the spurious signal originating from the cryogenic insert in the ESR cavity. The temperature dependence of the linewidth  $\Delta H$  is shown in the main panel of Fig. 3. The linewidth  $\Delta H$  slightly decreases with decreasing temperature from 0.1 T

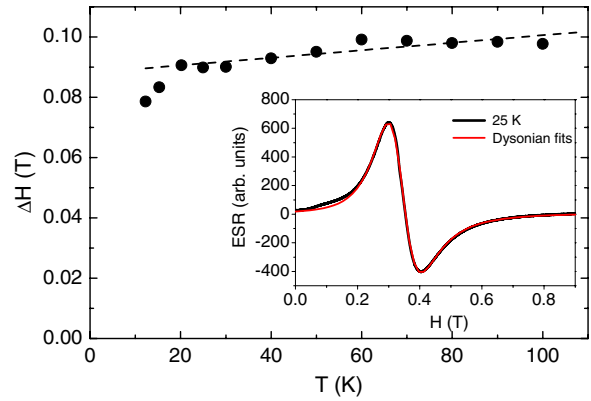


FIG. 3. (Color online) The temperature of the ESR linewidth  $\Delta H$  of the  $\text{EuCu}_2\text{Si}_2$  single crystal. The dashed line is a linear fit  $\Delta H = A + BT$  in the temperature range of 20–100 K. The inset shows the measured ESR line at 25 K (solid line) and a corresponding fit (dashed line) to a Dysonian function (see the text).

( $T = 100$  K) to 0.08 T ( $T = 10$  K). The linear dependence  $\Delta H = A + BT$  (for the fit see Fig. 3) indicates that the spin relaxation of localized moments is due to the exchange interaction with conduction electrons via a so-called Korringa mechanism.<sup>21</sup> The fit yields  $B \sim 1.25 \cdot 10^{-4}$  T/K for the Korringa slope, which is similar to the result obtained in Ref. 12. In contrast to that work we observed a much larger residual linewidth ( $A \sim 0.088$  T). Since  $A$  is usually attributed to the temperature-independent inhomogeneous broadening, the large value of  $A$  suggests substantial chemical disorder of the studied sample. The measured  $g$  factor is  $g_{\parallel} \sim 2.011(3)$  in the temperature range of 10–100 K. The above listed observations strongly suggest that we observed the ESR of localized  $\text{Eu}^{2+}$  ions  $4f^7$  ( $J = S = 7/2$ ,  $L = 0$ ,  $g = 2$ ) which interact with conduction electrons. For temperatures below 7 K the measured spectra change dramatically and a line splitting evolves in decreasing temperature (Fig. 4). This evolution suggests the occurrence of an internal magnetic field at  $T < 7$  K possibly due to the development of short-range quasistatic magnetic correlations. This becomes also evident from the upturn of the magnetic susceptibility in this temperature range [Fig. 1(a)] and the onset of the low-temperature anomaly of  $C_p/T$  (inset to Fig. 5).

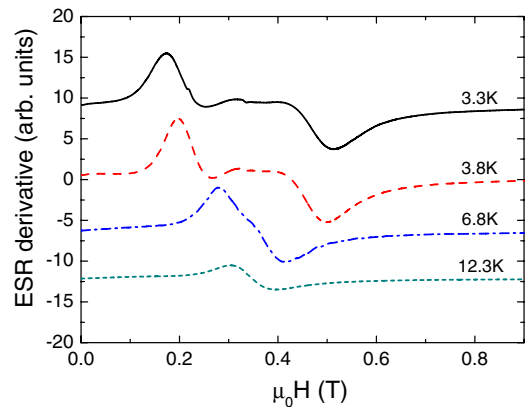


FIG. 4. (Color online) Selected ESR spectra of  $\text{EuCu}_2\text{Si}_2$  single crystal in the low-temperature range  $T = 3.3$  K to 12.3 K.

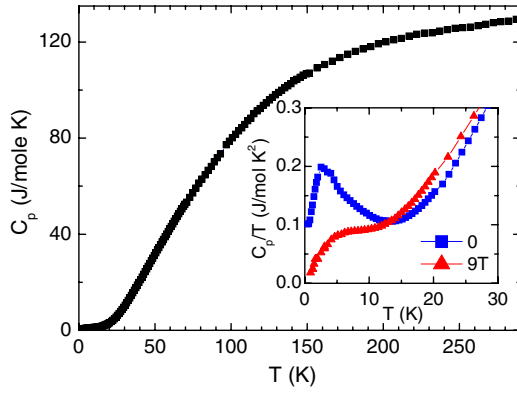


FIG. 5. (Color online) Specific heat as a function of temperature  $C_p(T)$  of a  $\text{EuCu}_2\text{Si}_2$  single crystal. Inset: specific heat  $C_p/T$  vs  $T$  in zero field (squares) and in an external magnetic field of 9 T (triangles), respectively.

### B. Specific heat

The specific heat  $C_p$  as a function of temperature between 0.5 and 290 K is shown in Fig. 5. The overall behavior of  $C_p(T)$  for single crystal differs qualitatively from that of polycrystals.<sup>3</sup> As visible in the inset to Fig. 5, in the temperature range  $T < 15$  K, there are striking additional entropy changes since the specific heat clearly deviated from a conventional Debye behavior. Instead, there is a distinct maximum at  $T \approx 2.5$  K, which deviates at least quantitatively from the broad and much larger anomaly of the magnetic specific heat observed in single crystals grown from the In flux.<sup>12</sup> In particular, there is no signature of a phase transition. Therefore, our data rule out long-range magnetic order in the crystal for  $T > 0.5$  K. One might speculate, however, whether these additional entropy changes have a similar, i.e., antiferromagnetic, nature as the entropy changes in the In flux-grown single crystal, which are related to the development of antiferromagnetic order at 10 K.<sup>8,22,23</sup>

Application of a magnetic field of 9 T leads to drastic changes in the specific heat. The low-temperature anomaly of  $C_p/T$  becomes completely suppressed, which proves the magnetic origin of the excess specific-heat contribution. Instead, in the presence of a high magnetic field  $C_p/T$  exhibits a sharp drop at  $T < 2.5$  K. On the other hand, the magnetic field yields an increase in the specific heat in the temperature range  $13 < T < 40$  K. Such a behavior supports the scenario that the zero-field anomaly might be related to short-range antiferromagnetic spin correlations, which are naturally suppressed in an external magnetic field. In contrast, at higher temperatures up to 40 K the specific-heat data imply a field-induced magnetic order, which will be discussed below in terms of the field-induced alignment of local  $\text{Eu}^{2+}$  spins forming stable magnetic moments.

### C. Electronic transport properties

The electrical resistivity vs temperature  $\rho(T)$  of single crystalline samples for two different axis orientations,  $c$  axis and  $a$  axis, is shown in Fig. 6. The plots have been normalized to the resistance at  $T = 295$  K. In contrast to the magnetic susceptibility, the anisotropy in the electrical resistivity

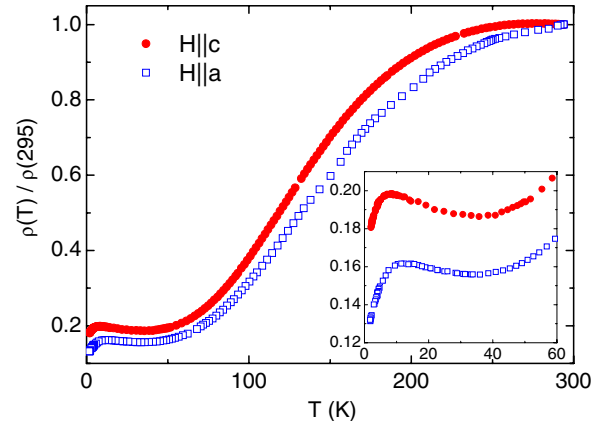


FIG. 6. (Color online) Normalized electrical resistivity  $\rho(T)/\rho(295 \text{ K})$  as a function of temperature parallel to  $a$  and  $c$  axes of  $\text{EuCu}_2\text{Si}_2$  single crystal. Inset: low-temperature region  $T < 60$  K.

for the two different crystallographic orientations is less significant. Parallel to the  $c$  axis  $\rho(295 \text{ K}) = 65 \mu\Omega \text{ cm}$  is slightly smaller than  $\rho(295 \text{ K}) = 90 \mu\Omega \text{ cm}$  parallel to the  $a$  axis. The temperature dependence is qualitatively similar to that of  $\text{EuCu}_2\text{Si}_2$  single crystals previously reported<sup>12,13</sup> and displays the typical sigmoid behavior between room temperature and He temperature (4.2 K). The residual resistance ratio  $\rho(5 \text{ K})/\rho(295 \text{ K}) \approx 15\%$  for our crystal is significantly larger than  $\approx 6\%$  in Ref. 12; however, it is much smaller than that reported in Ref. 13 [ $\rho(5 \text{ K})/\rho(295 \text{ K}) \approx 36\%$ ]. The specific resistivities,  $\rho(295 \text{ K}) = 65 \mu\Omega \text{ cm}$  in the present work vs  $68 \mu\Omega \text{ cm}$  in Ref. 12, are comparable whereas  $\rho(295 \text{ K}) = 220 \mu\Omega \text{ cm}$  was obtained in Ref. 13. Polycrystalline samples prepared with the nearly stoichiometric composition  $\text{Eu}_{20}\text{Cu}_{40}\text{Si}_{40}$  display similar temperature dependence  $\rho(T)$  as single crystal, whereas for off-stoichiometric composition the electrical resistivity is virtually constant. But the specific resistivity of most polycrystalline samples is one order of magnitude larger than that of single crystalline samples probably because of macroscopic defects (cracks, grain boundaries, and precipitates), which are absent in single crystals. Therefore, the behavior of polycrystals does not reflect intrinsic properties.

At low temperatures ( $T \approx 30$  K) a Kondo-like resistance anomaly in form of a small peak is visible before the resistivity drops at very low temperatures. This temperature evolution of the resistivity can be clearly seen on the magnified scale (inset to Fig. 6). In order to elucidate the nature of this anomaly, the longitudinal magnetoresistance (MR) in  $a$ -axis orientation was measured in magnetic fields up to 10 T (Fig. 7). A negative MR was observed for temperatures ( $T \approx 12$  K) close to the maxima of  $\rho(T)$  (inset to Fig. 7). For low temperatures ( $T \approx 1.8$  K) a transition from positive to negative MR was inferred. The Kondo-like anomaly is gradually suppressed with increasing magnetic field, which suggests its magnetic origin and implies that the short-range magnetic correlations may persist well above 2 K.

## IV. DISCUSSION

From magnetization and ESR measurements one can conclude that a sizable fraction of Eu ions in the studied single

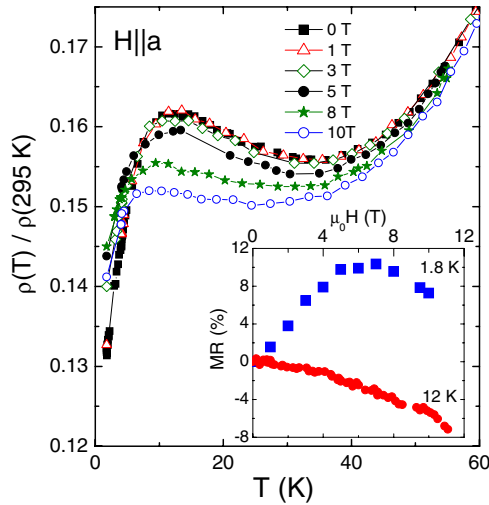


FIG. 7. (Color online) Normalized electrical resistivity  $\rho(T)/\rho(295\text{ K})$  as a function of temperature of  $\text{EuCu}_2\text{Si}_2$  single crystal for external magnetic fields parallel to the  $a$  axis ( $\mu_0 H=0$  to 11 T). Inset: MR as a function of field at selected temperatures.

crystal possesses a stable magnetic moment associated with the spin  $S=7/2$  of  $\text{Eu}^{2+}$ . Their random distribution in the lattice is manifested in the large residual ESR line width and resistivity. One can conjecture that, owing to the interaction of these local states with conduction electrons which is evidenced by a Korringa relaxation broadening of the ESR signal, a partial Kondo-like screening of the local spins can occur at low temperatures. An indication for that could be an upturn in the resistivity below  $\sim 30$  K followed by its downturn at  $T < 7$  K. The former can be assigned to the enhanced scattering of the itinerant electrons on the  $4f$ -local states, whereas the latter can be due to the formation of the coherent Kondo state. However, if a Kondo-like state indeed takes place, the Kondo screening is obviously noncomplete. Apparently there is a competing magnetic ground state of an antiferromagnetic nature whose signatures at low temperatures are visible in magnetization and ESR data. In this situation a strong impact of the external magnetic field on the resistivity and the specific heat is not surprising. It can be understood as a breakdown of the Kondo-like state in favor of a magnetic state with a fully restored  $4f$  moment. For example, under these conditions a similar sign reversal of the MR (inset to Fig. 7) and the shift of the magnetic entropy to higher temperatures were observed in the heavy fermion compound  $\text{YbRh}_2\text{Si}_2$  (see Ref. 24).

The considerable distinction of magnetic properties between  $\text{EuCu}_2\text{Si}_2$  polycrystalline samples and crystals synthesized by diverse preparation routes has been attributed to a

particular chemical defect structure (rather than to impurities).<sup>6,12</sup> This is evident from different lattice parameters of samples reported in various references. Their summary is given in Table I. The polycrystalline specimens exhibit a relatively small unit-cell volume  $V=a^2c$ .<sup>12,25</sup> The lattice parameters and the unit-cell volume  $V=0.1639\text{ nm}^3$  of the FZ-grown single crystal studied here resemble those of polycrystals. In contrast, the  $a$  axis and unit-cell volumes,  $V=0.1685\text{ nm}^3$  (Ref. 12) and  $V=0.1669\text{ nm}^3$ ,<sup>13,18</sup> of crystals grown from In flux are considerably larger.

It is supposed that different effective valence states of Eu exist in the various specimens. The presence of a small fraction of  $\text{Eu}^{2+}$  ions in the FZ-grown crystal inferred from our magnetic measurements is supported by the ESR spectra. Because the ionic radius of divalent  $\text{Eu}^{2+}$  is substantially larger than trivalent  $\text{Eu}^{3+}$ , the observed smaller unit-cell volume of the FZ-grown crystal (compared to those grown from an In flux) is consistent with a larger fraction of the trivalent nonmagnetic configuration  $\text{Eu}^{3+}$ .<sup>17</sup> The reduced fraction of magnetic  $\text{Eu}^{2+}$  ions may explain the lack of any magnetic transition at  $T > 2$  K both in polycrystals and in the FZ-grown crystal studied. Instead, spin fluctuations are observed for low temperatures, which can also give rise to Kondo-like resistance anomalies. This behavior contrasts with the antiferromagnetic ordering at  $T_N=10$  K in  $\text{EuCu}_2\text{Si}_2$  single crystals synthesized from the In flux.<sup>12,13</sup> Only recently, Stadnik *et al.*<sup>18</sup> found out by Mössbauer measurements that the  $\text{EuCu}_2\text{Si}_2$  single crystals grown from the In flux do not show any charge fluctuations but exhibit a stable  $\text{Eu}^{2+}$  state. Also studies performed on  $\text{EuCu}_2\text{Ge}_2$  and doped  $\text{EuCu}_2(\text{Si}_x\text{Ge}_{1-x})_2$  proved the stabilization of divalent  $\text{Eu}^{2+}$  and a magnetically ordered phase through the substitution of Si by Ge (with a larger ionic radius).<sup>13,26,27</sup>

We assume that the primary origin of the remarkable differences in properties and lattice parameters of  $\text{EuCu}_2\text{Si}_2$  crystals from different preparation methods are small composition variations. A direct comparison of crystals is not viable because of the lack of composition data in Refs. 12 and 13. However, the typical energy dispersive x-ray analysis of our FZ-grown crystal, 21.8 at. % Eu, 39.7 at. % Cu, and 38.6 at. % Si, not only proved a slight excess of Eu but also a depletion in Cu and Si compared to the  $\text{Eu}_{20}\text{Cu}_{40}\text{Si}_{40}$  stoichiometry. Bearing in mind this stoichiometry deviation, a Rietveld analysis of the structure data was performed. It is consistent with a  $\text{ThCr}_2\text{Si}_2$ -type structure where excess Eu ions can randomly occupy Cr sites (normally occupied by Cu ions) and a small fraction of Cu ions on Si sites. This is the origin of chemical disorder also inferred from the ESR measurements.

In Ref. 6, it was argued that a Si-rich surrounding should promote the divalent  $\text{Eu}^{2+}$ ; therefore, the Si-depleted compo-

TABLE I. Lattice constants of  $\text{EuCu}_2\text{Si}_2$  specimen for various preparation conditions.

Parameter	Powder Ref. 25	Polycrystal Ref. 12	Single crystal Ref. 12	Single crystal Refs. 13 and 18	Single crystal (Present work)
$a$ (nm)	0.407	0.408–0.405	0.4111	0.410	0.4061(1)
$c$ (nm)	0.993	0.996	0.9968	0.993	0.9936(1)
$V=a^2c(\text{nm}^3)$	0.1645	0.1658–0.1634	0.1685	0.1669	0.1639

sition obtained rather supports the preference of  $\text{Eu}^{3+}$  ions. However, the explanation of the observed behavior on an atomic level is beyond the scope of the present paper. As mentioned above, the observed dependence of physical behavior on the preparation route is typical for  $\text{ThCr}_2\text{Si}_2$ -type compounds.<sup>14</sup> It finally originates from slight differences in composition. Exact composition data of specimen studied are scarce. Only recently it was found that the homogeneity range of another  $\text{ThCr}_2\text{Si}_2$ -type compound  $\text{ErPd}_2\text{Si}_2$  extends over 6 at. %.<sup>28</sup> This may explain the observed diversity of properties of this class of compounds as a function of preparation method. The comparison of single crystals synthesized in different ways, instead of polycrystalline samples as in the majority of studies of  $\text{ThCr}_2\text{Si}_2$ -type rare-earth compounds, proved that the variation of properties is intrinsic in nature but not primarily caused by defects.

## V. CONCLUSIONS

We have presented the results of magnetization, ESR, specific-heat, and resistivity measurements on  $\text{EuCu}_2\text{Si}_2$

single crystals. While the magnetic behavior is anisotropic with an easy  $c$  axis, no magnetic ordering transition was observed at  $T > 2$  K. The data provide evidence for a mixed-valence behavior and short-range magnetic correlations at low temperatures concomitant with a Kondo-like behavior. Finally, we conclude that the diversity of the physical properties as a consequence of the particular preparation route employed for single crystals and polycrystals results from different lattice parameters and chemical disorder, which are characteristic for classes of intermetallic compounds with a wide homogeneity range.

## ACKNOWLEDGMENTS

The authors thank S. Pichl, S. Mueller-Litvanyi, A. Ostwaldt, J. Werner, and R. Mueller for experimental assistance and W. X. Zhang for helpful discussions. Some authors express their gratitude for the financial support under Grant No. SFB 463 of the Deutsche Forschungsgemeinschaft (V.K., W.L., and G.B.), the Alexander von Humboldt-Stiftung (C.D.C. and F.M.), and the NSF of China and NPU-FIST (C.D.C.).

- 
- <sup>1</sup>A. Szytuła and J. Leciejewicz, in *Handbook on the Physics and Chemistry of Rare Earths*, edited by K. A. Gschneider, Jr. and L. Eyring (Elsevier, Amsterdam, 1989), Vol. 12, p. 133.
- <sup>2</sup>A. Szytuła and J. Leciejewicz, *Handbook on Crystal Structures and Magnetic Properties of Rare Earth Intermetallics* (CRC, Boca Raton, 1994), p. 151.
- <sup>3</sup>B. C. Sales and D. K. Wohlleben, *Phys. Rev. Lett.* **35**, 1240 (1975).
- <sup>4</sup>B. C. Sales and R. Viswanathan, *J. Low Temp. Phys.* **23**, 449 (1976).
- <sup>5</sup>E. V. Sampathkumaran, L. C. Gupta, and R. Vijayaraghavan, *Phys. Rev. Lett.* **43**, 1189 (1979).
- <sup>6</sup>A. Scherzberg, Ch. Sauer, U. Köbler, W. Zinn, and J. Röhler, *Solid State Commun.* **49**, 1027 (1984).
- <sup>7</sup>P. A. Alekseev, R. V. Chernikov, K. V. Klementiev, V. N. Lazukov, and A. P. Menushenkov, *Nucl. Instrum. Methods Phys. Res. A* **543**, 202 (2005).
- <sup>8</sup>E. R. Bauminger, D. Froindlich, I. Nowik, and S. Ofer, *Phys. Rev. Lett.* **30**, 1053 (1973).
- <sup>9</sup>K. J. H. Buschow, M. Campagna, and G. K. Wertheim, *Solid State Commun.* **24**, 253 (1977).
- <sup>10</sup>T. V. Ramakrishnan and K. Sur, *Phys. Rev. B* **26**, 1798 (1982).
- <sup>11</sup>R. Mock, B. Hillebrands, H. Schmidt, G. Guentherodt, Z. Fisk, and A. M. Meyer, *J. Magn. Magn. Mater.* **47-48**, 312 (1985).
- <sup>12</sup>P. G. Pagliuso, J. L. Sarrao, J. D. Thompson, M. F. Hundley, M. S. Sercheli, R. R. Urbano, C. Rettori, Z. Fisk, and S. B. Oseroff, *Phys. Rev. B* **63**, 092406 (2001).
- <sup>13</sup>J. S. Rhyee, B. K. Cho, and H. C. Ri, *J. Appl. Phys.* **93**, 8346 (2003).
- <sup>14</sup>S. L. Bud'ko, Z. Islam, T. A. Wiener, I. R. Fisher, A. H. Lacerda, and P. C. Canfield, *J. Magn. Magn. Mater.* **205**, 53 (1999).
- <sup>15</sup>G. Behr, W. Löser, D. Souptel, G. Fuchs, I. Mazilu, C. Cao, A. Köhler, L. Schultz, and B. Büchner, *J. Cryst. Growth* **310**, 2268 (2008).
- <sup>16</sup>E. M. Levin, B. S. Kuzhel, O. I. Bodak, B. D. Belan, and I. N. Serts, *Phys. Status Solidi B* **161**, 783 (1990).
- <sup>17</sup>S. Patil, R. Nagarajan, L. C. Gupta, C. Godart, R. Vijayaraghavan, and B. D. Padalia, *Phys. Rev. B* **37**, 7708 (1988).
- <sup>18</sup>Z. M. Stadnik, P. Wang, J. Zukrowski, and B. K. Cho, *Hyperfine Interact.* **169**, 1295 (2006).
- <sup>19</sup>R. Klingeler, B. Büchner, S.-W. Cheong, and M. Hücker, *Phys. Rev. B* **72**, 104424 (2005).
- <sup>20</sup>F. J. Dyson, *Phys. Rev.* **98**, 349 (1955).
- <sup>21</sup>J. Korringa, *Physica (Amsterdam)* **16**, 601 (1950).
- <sup>22</sup>G. R. Stewart, Z. Fisk, J. O. Willis, and J. L. Smith, *Phys. Rev. Lett.* **52**, 679 (1984).
- <sup>23</sup>K. Tsuchida, C. Kato, T. Fujita, Y. Kobayashi, and M. Sato, *J. Phys. Soc. Jpn.* **73**, 698 (2004).
- <sup>24</sup>P. Gegenwart, Y. Tokiwa, T. Westerkamp, F. Weickert, J. Custers, J. Ferstl, C. Krellner, C. Geibel, P. Kersch, K.-H. Müller, and F. Steglich, *New J. Phys.* **8**, 171 (2006).
- <sup>25</sup>*Pearsons Handbook of Crystallographic Data for Intermetallic Phases*, 2nd ed., edited by P. Villars and L. D. Calvert (ASM, Metal Park, OH, 1991), Vol. 3, p. 2801.
- <sup>26</sup>E. M. Levin, T. Palewski, and B. S. Kuzhel, *Physica B (Amsterdam)* **294-295**, 267 (2001).
- <sup>27</sup>Z. Hossain, C. Geibel, N. Senthilkumaran, M. Deppe, M. Baenitz, F. Schiller, and S. L. Molodtsov, *Phys. Rev. B* **69**, 014422 (2004).
- <sup>28</sup>I. Mazilu, A. Teresiak, J. Werner, G. Behr, C. D. Cao, W. Löser, J. Eckert, and L. Schultz, *J. Alloys Compd.* **454**, 221 (2008).